Phytoplankton microstructure in fully developed oceanic turbulence

Hidekatsu Yamazaki,[1] James G. Mitchell,[2] Laurent Seuront,[2,3] Fabian Wolk,[4] and Hua Li[5]

Received 24 July 2005; revised 23 November 2005; accepted 30 November 2005; published 6 January 2006.

[1] Turbulence alters phytoplankton distributions. In doing so, it changes light and nutrient availability that ultimately influences community composition and carbon flux. The quantitative basis for this paradigm is the matching of the $-5/3$ slopes of fluorescence and velocity spectra over scales ranging from 1 to 100 m. In this contribution, for the first time, we simultaneously show the $-5/3$ spectral slopes for velocity and fluorescence at sub-metre scales. The fluorescence spectral slopes deviate from the $-5/3$ slope with less steep slopes, suggesting the existence of a viscous-convective subrange for fluorescence. However, it is difficult to identify the -1 slope as predicted by the Batchelor spectral theory. This portion of spectrum could be white as proposed by Franks (2005). High order structure functions indicate that the fluorescence is more intermittent than the velocity, but less intermittent than the conductivity signals.). **Citation:** Yamazaki, H., J. G. Mitchell, L. Seuront, F. Wolk, and H. Li (2006), Phytoplankton microstructure in fully developed oceanic turbulence, *Geophys. Res. Lett.*, *33*, L01603, doi:10.1029/2005GL024103.

1. Introduction

[2] The prediction and confirmation that the power spectrum for velocity fluctuations in a turbulent fluid fits a $-5/3$ slope between the energy input scale and the viscous cutoff scale, namely the inertial subrange, is one of the most significant and robust achievements in fluid dynamics of the last century [*Frisch*, 1995; *Pope*, 2000]. Phytoplankton are widely acknowledged to trace water movement and thus expected to exhibit the same $-5/3$ slope as water velocity over the inertial subrange. For scales greater than the inertial subrange, which are the length scales over which turbulent energy cascades to progressively smaller scales, phytoplankton cease tracing water movement and form patches because their growth rates are faster than the dispersion from mixing. For scales from the inertial subrange downward, turbulent mixing is assumed to be an effective homogenizer of fluorescence distributions, but this has not been established below distances of 1 m [*Denman et al.*, 1977; *Powell and Okubo*, 1994]. However, interactions among plankton take place well below this scale, and little is known about the extent to which these interactions structure phytoplankton distributions at this scale. Here, we report the relationship between fully developed turbulence and phytoplankton distributions at scales from a meter down to a centimeter to determine the extent and nature of any general spatial relationships.

2. Measuring Biophysical Microstructures

[3] To obtain a representative picture of phytoplankton distributions, high-resolution sampling of undisturbed water is needed. The fluorescence signal from chlorophyll is commonly used as a measure of phytoplankton abundance [*Platt*, 1972; *Denman and Gargett*, 1995]. However, this signal is usually contaminated by oscillations of the instrument caused by the tether to the ship, protective cages around sensors, blunt-end sensor design and the shape of the excitation and detection volumes. To circumvent these problems, we used a free-fall vertical profiler (TurboMAP) that was specifically designed for concurrent measurements of turbulent parameters (velocity shear, $\partial u/\partial z$, where u and z are the turbulent fluctuating cross-stream velocity component and the depth, respectively), hydrographic parameters (pressure, temperature and conductivity) and bio-optical parameters (in vivo fluorescence and backscatter [*Wolk et al.*, 2002]). All sensors are set onto a parabolically shaped cap at the head of the instrument. This arrangement ensures these sensors are in an undisturbed flow. All signals are simultaneously sampled at 256 Hz and stored internally in a memory card. The design of the instrument minimizes interference from the problems mentioned above.

[4] We have developed a new LED fluorescence probe to provide high spatial resolution of the fluorescence field. Great care was taken in investigating the spatial transfer function of the LED probe. We towed the LED probe and a high response thermistor (FP07) at a constant speed (0.1 m/s) in a laboratory channel to estimate the spatial transfer function of the LED probe using the known spatial response of the FP07 probe [*Wolk et al.*, 2006]. Since the turbulent velocity spectrum can be corrected using a single pole transfer function [*Oakey*, 1982] and compared with the Nasmyth empirical spectrum [*Nasmyth*, 1970], the fluorescence signals can be faithfully compared with the velocity field.

[5] We made observations off of the Japanese coast in the Neko Seto Sea (34°10′N, 132°30′E) during daytime in mid-August. The well-mixed water column chosen here minimizes the masking of microscale distributions by macroscale features, such as strong pycnoclines. In this region, tidal flow up to 1.8 m s^{-1} creates a well-mixed water column [*Takasugi et al.*, 1994], where temperature variation is less than 0.1°C over the whole depth (Figure 1). Since the water column is well mixed, the buoyancy frequency is in the order of 10^{-3} (s^{-1}). The profile average dissipation rate is 1.46×10^{-7} (W kg^{-1}). The data show the combination of

[1]Department of Ocean Sciences, Tokyo University of Marine Science and Technology, Tokyo, Japan.
[2]Biological Sciences, Flinders University of South Australia, Adelaide, South Australia, Australia.
[3]Station Marine de Wimereux, CNRS UPRESA 8013 ELICO, Université des Sciences et Technologies de Lille, Wimereux, France.
[4]Rockland Oceanographic Services Inc., Victoria, British Columbia, Canada.
[5]Alec Electronics Co., Kobe, Japan.

0094-8276/06/2005GL024103$05.00

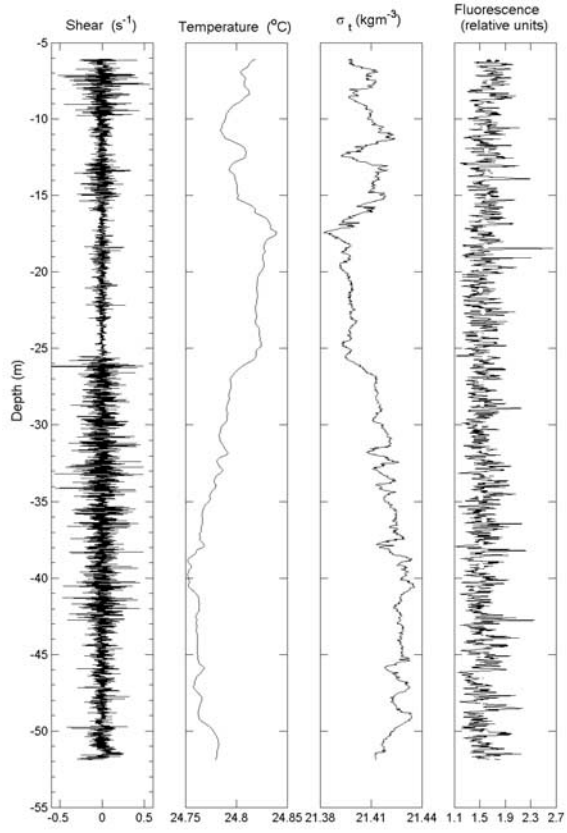

Figure 1. Microstructure data obtained from TurboMAP. The water column is fully turbulent according to shear data, salinity and density. The water column is well mixed, as the turbulence level indicates. With a 2 mm sampling interval the fluorescence signal is intermittent. In comparison, the same data averaged over 1.5 meter is similar to that provided by standard CTD protocols in that it does not change significantly (circles) and so misses the intermittency, implying a homogeneous phytoplankton distribution. This is in direct contrast to the local phytoplankton distribution structure presented here.

both micro (<1 m) and fine scale (>1 m) fluctuations of shear, temperature, density (σ_T) and in vivo fluorescence signals. More specifically, in vivo fluorescence signals show large excursions that can reach values of up to 86% of the mean. The reality of these microscale fluctuations has been demonstrated elsewhere [*Wolk et al.*, 2004].

[6] Numerous density inversions appear in the density profile and are consistent with the observed dissipation rate. In these turbulent conditions, water movement over centimeters to meters is isotropic. Consequently, the geometry of local fluorescence peaks are likely to be closer to short ribbons or small pancakes, rather than the extensive layered sheets that appear at density interfaces, and so we infer that small peaks in our data represent micropatches.

3. Spectra and Structure Functions

[7] *Kolmogorov* [1941] proposed one of the most successful theories in the area of turbulence study, namely the velocity spectrum, $E(k)$, for fully developed turbulence should be expressed as $E(k) = C\varepsilon^{2/3} k^{-5/3}$, where k is the wavenumber, ε the rate of kinetic energy dissipation and C a universal constant. The power spectrum drops sharply in the viscous dissipation range, but maintains a universal form. *Nasmyth* [1970] experimentally derived the universal spectrum that has been widely used to compare with measured spectra in the oceanography community.

[8] When the kinematic viscosity ν of a fluid is much larger than the diffusivity κ_θ of a scalar θ so the Schmidt number $Sc = \nu/\kappa_\theta$ is large, fluctuation in the scalar field persists at higher wavenumbers than those of velocity. This range is called the viscous-convective subrange that shows a k^{-1} spectral slope. *Batchelor* [1959] proposed a spectrum for the viscous-convective regime ($\eta^{-1} \ll k \ll \eta_B^{-1}$) given by $\phi(k) = B\chi_\theta(\nu/\varepsilon)^{1/2} k^{-1}$, where B is the Batchelor constant, $\eta = (\nu^3/\varepsilon)^{1/4}$ the Kolmogorov length scale, $\eta_B = \eta Sc^{-1}$ the Batchelor scale and χ_θ the dissipation rate of scalar variance. When the Reynolds number of the flow is high, the scalar spectrum may show an inertial-convective subrange in $k \ll \eta_B^{-1}$, and is given by $\phi(k) = \beta\chi_\theta\varepsilon^{-1/3} k^{-5/3}$, where β is a universal constant [*Corrsin*, 1951].

[9] The normalized velocity spectra (Figure 2) show a conventional inertial subrange (roughly between 3 and 30 cpm). The average dissipation rate of turbulent kinetic energy is 3×10^{-7} W kg^{-1}. The velocity spectra are normalized in wavenumber by the Kolmogorov scale, which is of order of 10^{-3} m (Table 1). At this scale, almost all the kinetic energy is lost to viscosity. The low wavenumber portion of the fluorescence spectrum is flat, suggesting that the phytoplankton distribution is well mixed at this scale. We fit linear slopes to the inertial subrange and

Table 1. Average Dissipation Rates and the Corresponding Kolmogorov Scale for Each Profile[a]

Profile	$\varepsilon \times 10^{-7}$, W kg^{-1}	$\eta \times 10^{-3}$, m	Inertial Subrange Slope	Viscous-Convective Subrange Slope
1	3.25	1.26	−1.67	−0.51
2	7.85	1.01	−1.71	0.12
3	3.49	1.24	−1.43	−1.47
4	1.46	1.54	−1.98	0.57
5	0.87	1.75	−1.16	−1.08
7	5.67	1.10	−1.36	0.29
8	0.78	1.80	−1.80	−0.74

[a]Linear regression is applied to both inertial subrange and the viscous-convective subrange (high wavenumber regime) to estimate the spectral slope in log-log scale. The inertial subrange shows consistent slope, but the viscous-convective subrange shows erratic feature and the slopes are not statistically different from zero slope (white) at a 5% significant level. Profile 6 was unsuitable for analysis due to data acquisition inconsistencies.

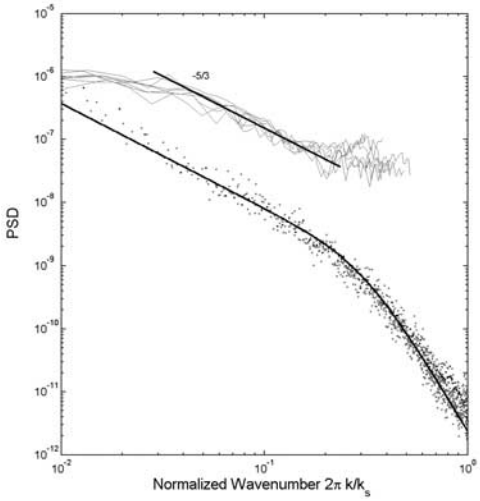

Figure 2. Composite power spectra for velocity (dotted) and fluorescence (thin solid line). The power spectrum for velocity is normalized by the Kolmogorov scaling in order to compare the empirical universal spectrum (thick solid line). The power spectrum of fluorescence is shown with the normalized wavenumber as that of the velocity, but the vertical coordinate is in arbitrary units. The thick straight line is the power spectra for fluorescence data and shows a −5/3 slope. Clearly, both fluorescence and turbulent velocity spectra exhibit the −5/3 slope in the same wavenumber range.

the viscous-convective subrange (Table 1). The fluorescence spectra agreed with the −5/3 slope in the inertial subrange, but the high wavenumber part does not show any consistent slope. The slopes range from a reverse cascade characterized by a positive slope to a slope typical of a viscous convective subrange. This indicates multiple driving processes at these scales, showing more complicated dynamics than demonstrated in the inertial subrange and more complicated than expected for the viscous convective subrange. *Franks* [2005] proposed that intermittent feature of fluorescence signals induces a white spectrum in high wavenumbers. However, the high variability found in the present work for the high-wavenumber part of the fluorescence spectra (see Table 1) suggests that it is still too early to lead a general conclusion about the high wavenumber slope of the fluorescence spectrum. More work is needed to confirm any prediction the specific expected slope in the viscous convective subrange.

[10] However, following *Li and Yamazaki* [2001], who fitted the Batchelor spectrum to high-resolution temperature data to estimate the dissipation rate of heat, we showed that one of the spectra followed the Batchelor spectrum (Figure 3). This Batchelor spectrum suggests an apparent diffusivity for the fluorescence field is about 10^{-8} m^2 s^{-1}. This value is smaller than the molecular thermal diffusivity (ca. 10^{-7} m^2 s^{-1}) and is larger than the molecular diffusivity of salt (10^{-9} m^2 s^{-1}). This apparent diffusivity for fluorescence suggests that phytoplankton microscale structure can potentially persist on a longer time scale than temperature structures, but less that that of salinity.

[11] According to the refined similarity hypothesis for a tracer [*Monin and Yaglom*, 1975] not only should the spectral shape for the tracer match the spectral shape for the velocity, but it should also exhibit intermittency in the viscous range. This has been confirmed for temperature [*Pumir*, 1994; *Lian-Ping et al.*, 1999], but not for phytoplankton. To measure the degree of intermittency we use the qth order structure functions for turbulent velocity, u, and scalar signal, θ, as $\langle [u(z+l) - u(z)]^q \rangle \approx l^{\zeta_u}(q)$ and $\langle [\theta(z+l) - \theta(z)]^q \rangle \approx l^{\zeta_u}(q)$, where "$\langle\ \rangle$" indicate the average quantity, z the vertical coordinate, l the separation distance between z and $(z + l)$. ζ_u and ζ_θ are the scaling exponent of the structure function for turbulent velocity and scalar signal. We examined fluorescence, F, and conductivity, C, as proxies of phytoplankton chlorophyll concentration and seawater density, respectively. The exponents $\zeta(q)$ are linear for Kolmogorov-Obukhov non-intermittent turbulence ($\zeta(q) = q/3$) and for a passive scalar advected by turbulent fluid motions ($\zeta(q) = qH$) [*Seuront et al.*, 1996a, 1996b, 1999], where H is given by $H = \zeta(1)$ and characterizes the degree of non-conservation of the mean process. In contrast, they are nonlinear and convex for intermittent processes and the intermittency is proportional to the convexity. Thus, ζ_u, ζ_F and ζ_C (Figure 4) indicate the signals are intermittent, with the greater convexity of ζ_F compared to ζ_u demonstrating that fluorescence is more intermittent than velocity fluctuation ($\zeta_F < \zeta_u$). However, the fluorescence signal is less intermittent than the conductivity signal ($\zeta_C > \zeta_F$).

[12] The significance of being able to measure the fluorescence intermittency and compare it to the velocity and conductivity intermittency from the same profile is that the biological distribution dynamic can now be followed in a

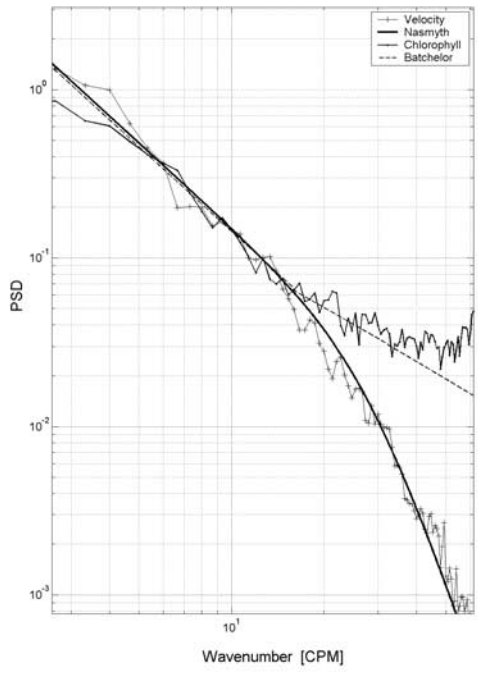

Figure 3. An estimation of apparent diffusivity for phytoplankton is attempted from the viscous-convective subrange theory [*Gibson and Schwartz*, 1963]. We used the Batchelor spectrum formula (dotted line) [*Oakey*, 1982] to fit the observed fluorescence spectrum (solid dot line). The power spectrum of velocity (solid cross line) is compared to the universal Nasmyth spectrum (solid line).

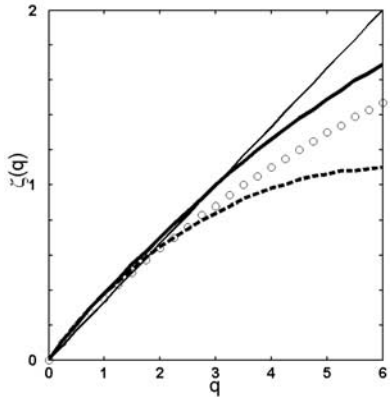

Figure 4. Higher order structure functions for velocity (thick line), fluorescence (open circle) and conductivity (dotted line) depart from a non-intermittent $q/3$ (straight line). Fluorescence is more intermittent than velocity, but is less intermittent than conductivity.

way that allows assessment of its response to physical oceanographic conditions. For future research, it is desirable to extend our knowledge to understanding how the intermittency changes with changes in nutrients, light, depth and wind.

4. Conclusion

[13] We have demonstrated the inertial subrange for fluorescence signal can exhibit a $-5/3$ slope in accordance with the conventional velocity spectrum. At high wavenumber the slope departs from the $-5/3$ in a variety of ways, demonstrating the potentially complex dynamics at these scales. The combined results of the fluorescence intermittency and the apparent diffusivity indicate that detectable structures in the fluorescence signals are smaller than the local structures of velocity field. The implication is that the intermittency and diffusion of the fluorescence signal are distinct from the other commonly measured physical parameters of velocity, temperature and conductivity. Most importantly, it was demonstrated that the fluorescence field diffusivity and intermittency can be estimated down to the dissipative range at high resolution, providing an opportunity for investigating phytoplankton dynamics in new ways. The availability of new high-resolution in-situ instrumentation lays the groundwork for unraveling the potentially complicated interactions among physical forcing, phytoplankton dynamics, zooplankton forcing and ultimately biogeochemical fluxes.

[14] **Acknowledgment.** This work was support by a Grant-in-Aid for Science Research (B2) 16310005 from Japan Society for the Promotion of Science and by grants from the Australian Research Council and Flinders University.

References

Batchelor, G. K. (1959), Small-scale variation of convected quantities like temperature in a turbulent fluid, part 1, *J. Fluid Mech.*, *XX*, 113–133.

Corrsin, S. (1951), On the spectrum of isotropic temperature fluctuations in isotropic turbulence, *J. Appl. Phys.*, *22*, 469–473.

Denman, K. L., and A. E. Gargett (1995), Biological-physical interactions in the upper ocean: The role of vertical and small scale transport processes, *Annu. Rev. Fluid Mech.*, *27*, 225–255.

Denman, K. L., A. Okubo, and T. Platt (1977), The chlorophyll fluctuation spectrum in the sea, *Limnol. Oceanogr.*, *22*(6), 1033–1038.

Franks, P. J. S. (2005), Plankton patchiness, turbulent transport and spatial spectra, *Mar. Ecol. Prog. Ser.*, *294*, 295–309.

Frisch, U. (1995), *Turbulence: The Legacy of A. N. Kolmogorov*, 296 pp., Cambridge Univ. Press, New York.

Gibson, C. H., and W. H. Schwarz (1963), The universal equilibrium spectra of turbulent velocity and scalar fields, *J. Fluid Mech.*, *16*, 365–384.

Kolmogorov, A. N. (1941), The local structure of turbulence in incompressible viscous fluid for very large Reynolds numbers, *Dokl. Akad. Nauk SSSR*, *30*, 299–303.

Li, H., and H. Yamazaki (2001), Observations of a Kelvin-Helmholtz billow in the ocean, *J. Oceanogr.*, *57*, 709–721.

Lian-Ping, W., S. Chen, and J. G. Brasseur (1999), Examination of hypotheses in the Kolmogorov refined turbulence theory through high-resolution simulations. part 2. Passive scalar field, *J. Fluid Mech.*, *400, 163–197.*

Monin, A. S., and A. M. Yaglom (1975), *Statistical Fluid Mechanics, Mechanics of Turbulence*, vol. 2, MIT Press, Cambridge, Mass.

Nasmyth, P. W. (1970), Oceanic turbulence, Ph.D. dissertation, Univ. of B. C., Vancouver, B. C., Canada.

Oakey, N. S. (1982), Determination of the rate of dissipation of turbulent energy from simultaneous temperature and velocity shear microstructure measurements, *J. Phys. Oceanogr.*, *12*, 254–271.

Platt, T. (1972), Local phytoplankton abundance and turbulence, *Deep Sea Res.*, *19*, 183–187.

Pope, S. B. (2000), *Turbulent Flows*, 771 pp., Cambridge Univ. Press, New York.

Powell, T. M., and A. Okubo (1994), Turbulence, diffusion and patchiness in the sea, *Philos. Trans. R. Soc. London, Ser. B*, *343*, 11–18.

Pumir, A. (1994), Small-scale properties of scalar and velocity differences in three-dimensional turbulence, *Phys. Fluids*, *6*, 3974–3984.

Seuront, L., F. Schmitt, Y. Lagadeuc, D. Schertzer, S. Lovejoy, and S. Frontier (1996a), Multifractal structure of phytoplankton biomass and temperature in the ocean, *Geophys. Res. Lett.*, *23*, 3591–3594.

Seuront, L., F. Schmitt, S. Schertzer, Y. Lagadeuc, and S. Lovejoy (1996b), Multifractal intermittency of Eulerian and Lagrangian turbulence of ocean temperature and plankton fields, *Nonlinear Processes Geophys.*, *3*, 236–246.

Seuront, L., F. Schmitt, Y. Lagadeuc, D. Schertzer, and S. Lovejoy (1999), Multifractal analysis as a tool to characterize multiscale inhomogeneous patterns. Example of phytoplankton distribution in turbulent coastal waters, *J. Plankton Res.*, *21*, 877–922.

Takasugi, Y., T. Fujiwara, and T. Sugimoto (1994), Formation of sand banks due to tidal vortices around straits, *J. Oceanogr.*, *50*, 80–95.

Wolk, F., H. Yamazaki, L. Seuront, and R. G. Lueck (2002), A free-fall profiler for measuring bio-physical microstructure, *J. Atmos. Oceanic Technol.*, *19*, 780–793.

Wolk, F., L. Seuront, H. Yamazaki, and S. Leterme (2004), Comparison of biological scale resolution from CTD and microstructure measurements, in *Handbook of Scaling Methods in Aquatic Ecology: Measurement, Analysis and Simulation*, edited by Laurent Seuront and Peter G. Strutton, pp. 3–15, CRC Press, Boca Raton, Fla.

Wolk, F., H. Yamazaki, H. Li, and R. G. Lueck (2006), Calibrating the spatial response of bio-optical sensors, *J. Atmos. Oceanic Technol.*, in press.

H. Li, Alec Electronics Co., 7-2-3 Ibukidai-higashi, Nishi, Kobe 651-2242, Japan.

J. G. Mitchell and L. Seuront, Biological Sciences, Flinders University of South Australia, GPO 2100, Adelaide, SA 5001 Australia.

F. Wolk, Rockland Oceanographic Services Inc., Victoria, BC, Canada V9A 4B6.

H. Yamazaki, Department of Ocean Sciences, Tokyo University of Marine Science and Technology, 4-5-7 Minato, Tokyo 108-8477, Japan. (hide@s.kaiyodai.ac.jp)